

Monte Carlo simulations probing the liquid/vapour interface of water/hexane mixtures: adsorption thermodynamics, hydrophobic effect, and structural analysis

Mona S. Minkara ^a, Tyler Josephson ^{a,b}, Connor L. Venteicher^a, Jingyi L. Chen^a, Daniel J. Stein ^a, Cor J. Peters ^c and J. Ilja Siepmann ^{a,b}

^aDepartment of Chemistry and Chemical Theory Center, University of Minnesota, Minneapolis, MN, USA; ^bDepartment of Chemical Engineering and Materials Science, University of Minnesota, Minneapolis, MN, USA; ^cChemical Engineering Department, Khalifa University of Science and Technology, Petroleum Institute, Abu Dhabi, UAE

ABSTRACT

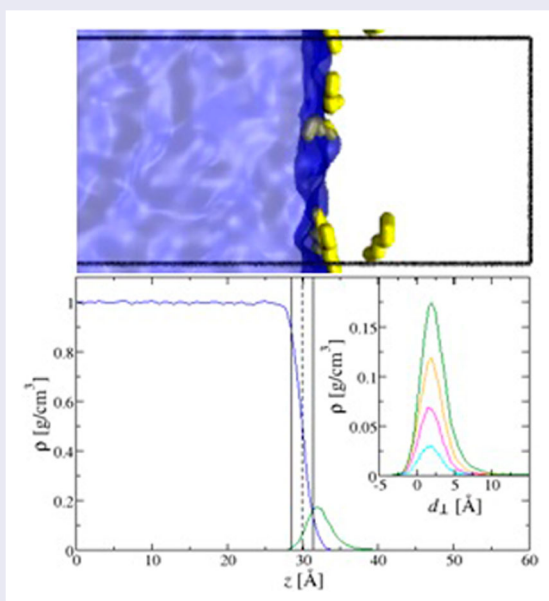
Knowledge about the interfacial properties of water/oil mixtures is important for the petrochemical industry and for understanding detergency and hydrophobic effects. Here, we probe the liquid/vapour interface of water/*n*-hexane mixtures using configurational-bias Monte Carlo simulations in the $N_W N_H V_W \rho_H T$ osmotic Gibbs ensemble. We study the effect of *n*-hexane at several partial pressures ranging from 25% to 95% of its saturated vapour pressure and observe that the surface tension decreases with increasing *n*-hexane pressure. Additionally, we analyse the simulation trajectories to provide molecular-level insights on the spatial distribution of *n*-hexane and the structure of the interface. The *n*-hexane molecules strongly adsorb from the vapour phase onto the liquid interface with a preferentially parallel orientation with respect to the interface. The surface excess, from the Gibbs adsorption isotherm equation, is calculated and used to systematically define the domain of adsorbed *n*-hexane. Integrating over this gives the free energy of adsorption of *n*-hexane, which is highly favourable, varying from -9.56 ± 0.03 to -10.40 ± 0.02 kJ/mol as the partial pressure of *n*-hexane is increased. The enrichment of *n*-hexane molecules on the interface yields a positive deviation from Henry's law at higher partial pressures, providing evidence for favourable adsorbate-adsorbate interactions.




ARTICLE HISTORY

Received 28 February 2018
Accepted 18 April 2018

KEYWORDS

Interface; surface tension; hydrophobic effect; adsorption; osmotic Gibbs ensemble



CONTACT J. Ilja Siepmann  siepmann@umn.edu  Department of Chemistry and Chemical Theory Center, University of Minnesota, 207 Pleasant Street SE, Minneapolis, MN 55455, USA;  Department of Chemical Engineering and Materials Science, University of Minnesota, 421 Washington Avenue SE, Minneapolis, MN 55455, USA

 Supplemental data for this article can be accessed at <https://doi.org/10.1080/00268976.2018.1471233>

1. Introduction

Hydrophobic effects at the liquid and vapour interface of water/oil mixtures are relevant to the petrochemical industry, the pharmaceutical industry, pesticides in agriculture, and drainage of water for transportation on highways [1–3]. Understanding the structure and thermodynamics of these interfaces can help mitigate the consequences of oil spills on the environment and climate, enhance oil recovery, improve hydraulic fracking, and provide insight into formation of seawater aerosols. One particularly interesting phenomenon is the wetting of alkanes to the air/water interface, in which alkanes maintain contact with the surface despite their immiscibility.

Researchers have conducted a number of experimental studies to understand the hydrophobic effect associated with water/oil surfaces [1,4–17]. For instance, Javadi *et al.* measured the adsorption of alkanes from the vapour phase using drop profile analysis tensiometry [15]. In this process, Javadi *et al.* formed a saturated alkane vapour atmosphere by placing a drop of water into a closed cuvette and then injecting the cuvette with an alkane/squalene mixture (typically 1 ml) after a set time (typically 300 s). After the injection, Javadi *et al.* observed an oil film form on the water droplet. The oil film caused the water surface tension to decrease in spite of the mixture's immiscibility [15]. In a similar experiment, Mucic *et al.* found that an increasing *n*-hexane composition (i.e. an increasing partial pressure) in the cuvette caused a corresponding decrease in the surface tension of water [17]. Even though one of the driving forces of the adsorption of *n*-hexane molecules from the vapour phase at the pure water surface is known to be the partial vapour pressure of the *n*-hexane vapour, Mucic *et al.* concluded that the mechanism is not well known [17].

While these experimental techniques can quantify the influence of hydrophobic vapour on the macroscopic surface tension of water, they have not yet explained the molecular mechanism behind these changes. Computational methods are well-suited for investigating such mechanisms because they provide molecular-level insight that experimental studies cannot. One such method, Molecular Dynamics (MD), was used before this work to examine the liquid/liquid interface of water and oil [18] and the liquid/vapour interface of water and surfactants [11].

Unlike MD and other computational methods, Monte Carlo (MC) simulations in the Gibbs ensemble allow particles to fluctuate between thermodynamically connected simulation boxes. This characteristic, unique to the MC method, is vital for quantifying the adsorption of alkanes onto an interface. Because of this feature, some have used

MC simulations to analyse the liquid/liquid interface of water and oil, while others have used them to examine the liquid/vapour interface of water and *n*-hexane [19]. Notably, Ashbaugh and Pethica used MC methods in the canonical ensemble to study the adsorption of methane and ethane at a liquid/vapour interface of water, but their analysis was limited by their small system sizes and simplified models that did not allow for the study of longer alkanes [10].

In this work, we leverage MC simulations in the osmotic Gibbs ensemble to model the adsorption of *n*-hexane onto a liquid water interface. Our aim is to provide molecular-level insight to expand upon the experimental findings of Javadi *et al.* [15] and Mucic *et al.* [17]. Our simulations involve a two-box system in which one box represents the isotropic vapour phase of *n*-hexane modelled by the TraPPE-UA force field, and the other box contains a liquid film of water, represented by the TIP4P/2005 water model with a constant surface area and applied normal pressure. Only the *n*-hexane molecules are allowed to transfer between the boxes, and the box containing the water slab is kept at a constant volume. With the adsorption of *n*-hexane at varying partial pressures, the change in surface tension of the water will validate the experimental findings.

2. Computational methods

In this work, the TraPPE-UA force field [20] and TIP4P/2005 water model [21] were used to represent *n*-hexane and water molecules, respectively. Specific bead definitions and their parameters are found in Tables S1–S4 in the Supporting Information (SI). All calculations were run using the in-house MCCCSC-MN (Monte Carlo for Complex Chemical Systems-Minnesota) software suite. Before the adsorption of *n*-hexane molecules onto a water slab was studied, two supporting calculations were performed.

First, the saturated vapour pressure of *n*-hexane was calculated at 297 K using MC simulations in the *NVT* Gibbs ensemble. These saturated vapour pressure calculations involved a two-box system where a pure liquid phase of 800 *n*-hexane molecules constituted one box, and a pure vapour phase of 200 *n*-hexane molecules constituted the other. Both boxes had a 15 Å cut off with tail corrections. In order to reach thermodynamic equilibrium, *n*-hexane molecules were allowed to undergo translation, rotation, and configurational-bias Monte Carlo (CBMC) moves. In this way, the two boxes were thermodynamically connected, allowing a total volume-conserving fluctuation move. This move was set to $2/N_{\text{molec}}$, where N_{molec} is the total number of molecules

in the system. Thirty per cent of the total moves between the two boxes were set to be particle transfers. When the system reached equilibrium, 16 independent simulations were performed with enough MC cycles to obtain a saturated vapour pressure with a standard error of the mean less than 0.5% of the value. From these simulations, the vapour pressure of hexane was found to be 41.1 ± 0.1 kPa (compared to experimental vapour pressure of 19.2 kPa [22]) and the liquid density was found to be 0.65955 ± 0.00004 g/cm³ (compared to experimental density of 0.6557 g/cm³ [22]). This overestimation of *n*-hexane's vapour pressure by the TraPPE-UA model is in agreement with previous simulations for *n*-pentane and *n*-octane, and the overprediction of the alkane vapour pressure and underprediction of the normal boiling point by about 10 K are known shortcomings of the relatively simple united-atom models [21]. To compare the simulated results with experiment and to ensure that the simulations correspond to stable two-phase systems, all further calculations are reported with respect to a reduced pressure of p/p_{sat} . In addition, because the vapour pressure of TIP4P/2005 is < 1 kPa at 297 K (i.e. about a factor of 4 smaller than the experimental value) [23], the contribution of water in the vapour phase is neglected, and all water in subsequent simulations is constrained to the box containing the interface.

Second, to procure a reference point for surface tension calculations, single-box *NVT* simulations were performed to calculate surface tension of neat water at 297 K. The box contained a pure liquid phase of 1800 water molecules with a 15 Å cutoff. Modified Janeček long range (JC) corrections [24] were implemented. After equilibration, the *z*-boxlength was doubled to obtain an interface, and 64 independent simulations were performed with enough MC cycles to obtain a surface tension with a standard error of the mean less than 5%. The surface tension, γ_{KB} , is calculated based on the Kirkwood and Buff definition [25,26]. The simulations are performed in an elongated (along the *z*-direction) box with periodic boundary conditions in all three directions that contains two liquid phases and two planar interfaces perpendicular to the *z*-direction. In this case, γ_{KB} can be determined as follows:

$$\gamma_{\text{KB}} = \frac{1}{2} \langle P_{\text{N}} - P_{\text{T}} \rangle L_z, \quad (1)$$

where L_z is the length of the periodic simulation box in the *z*-direction, P_{N} and P_{T} are the normal and tangential components, respectively, of the pressure tensor, and the factor of 1/2 accounts for the presence of two interfaces in the periodic box.

Adsorption isotherm data were calculated at four percentages (25, 50, 75, and 95%) of the saturated vapour pressure of *n*-hexane using the $N_{\text{W}}N_{\text{H}}V_{\text{W}}p_{\text{H}}T$

osmotic Gibbs ensemble, where the subscripts 'W' and 'H' refer to water and *n*-hexane, respectively. Two boxes were initialised; one contained a pure liquid phase of 1800 water molecules and the other contained a pure vapour phase of 50 *n*-hexane molecules. The liquid water box had a 15 Å cutoff with JC corrections, and the vapour *n*-hexane box had a cutoff equal to 20% of the boxlength with tail corrections. Using Lorentz–Berthelot (LB) combining rules with TraPPE-UA and TIP4P/2005 underestimates the cross-interaction between *n*-hexane and water because both models are non-polarisable and the *n*-hexane TraPPE-UA model does not carry partial charges. Consequently, we adopted the hydrophobic hydration (HH) alkane model for CH₃-O and CH₂-O cross interactions as developed by Ashbaugh *et al.* [27], who increased the respective ϵ_{ij} parameters by 3.5% and 3.8% and decreased their respective σ_{ij} parameters by 0.12% and 0.14%. These new parameters have been shown to improve the prediction of alkane hydration free energies [27]. Both the *n*-hexane and water molecules were allowed translation, rotation, and CBMC moves. Only the vapour box was allowed to fluctuate in volume, and the *n*-hexane molecules were the only particles allowed to transfer between the two boxes. After fully equilibrating the system, the *z*-boxlength of the water

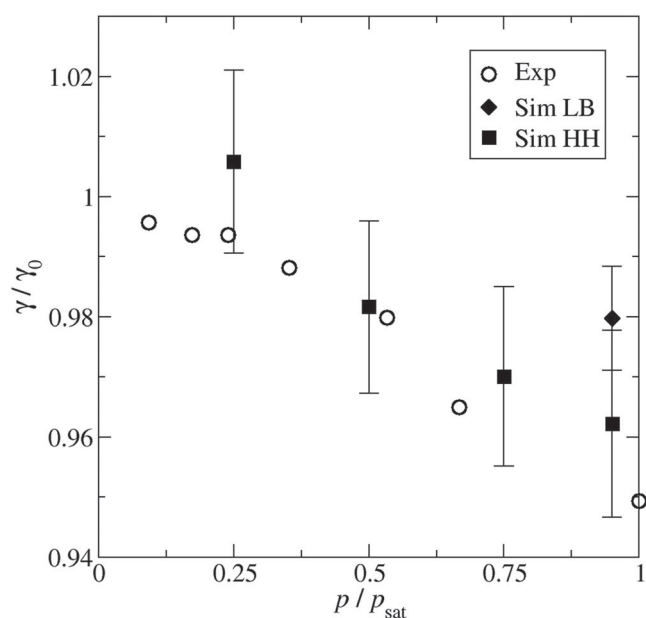


Figure 1. Calculated and experimental surface tensions of water as a function of *n*-hexane partial pressure, normalised to the surface tension of neat water. The diamonds and squares denote simulation data with water–hexane cross-interactions determined using the Lorentz–Berthelot combining rule (LB) and the hydrophobic hydration model (HH). Error bars are standard errors of the mean from 64 independent simulations.

Table 1. Distance and thickness of the interface for neat water and water in the presence of *n*-hexane vapour, as fit to Equation (2), as well as surface tensions calculated using Equation (1).

p/p_{sat}	$z_0(\text{\AA})$	$\xi(\text{\AA})$	$\gamma(\text{mN/m})$
–	30.09 ₅	2.85 ₂	69.5 ₃
0.25	29.972 ₈	2.84 ₃	70 ₁
0.50	30.000 ₅	2.91 ₂	68.2 ₉
0.75	30.00 ₂	2.95 ₃	67 ₁
0.95	29.942 ₆	2.94 ₁	67 ₁

box was doubled in order to obtain a interface. Sixty-four independent simulations were run with a sufficient amount of MC cycles to obtain a surface tension with a standard error of the mean less than 5%.

3. Results

3.1. Surface tension analysis

Figure 1 shows the experimental and simulated relative surface tensions of water with adsorbed *n*-hexane at each partial pressure, normalised to that of neat water. Absolute simulated surface tensions are given in Table 1. The surface tension of TIP4P/2005 water is 69.5 ± 0.3 mN/m at 297 K, consistent with a previously reported surface tension of 69.3 ± 0.9 mN/m at 300 K [21]. This is a 3% underestimation of the experimental surface tension of 71.5 mN/m. As the partial pressure of *n*-hexane vapour increases, the surface tension of the water decreases, in agreement with the experimental trend. Though the surface tension decreases for both the LB and HH σ_{ij} and ϵ_{ij} , the magnitude of the reduction is underestimated for the LB parameters and in agreement with experiment for the HH parameters developed by Ashbaugh *et al.* [27].

3.2. Defining the location of the interface

In order to characterise the position of the adsorbed *n*-hexane molecules with respect to the interface of the water slab, we must first determine the precise z -location and thickness of the interface. This interface is defined by fitting the density of water in z to Equation (2),

$$\rho(z) = \frac{1}{2}(\rho_{\text{liq}} + \rho_{\text{vap}}) - \frac{1}{2}(\rho_{\text{liq}} - \rho_{\text{vap}})\tanh\left(\frac{2(z - z_0)}{\xi}\right), \quad (2)$$

where ρ_{liq} is the average density of bulk water in the system (equal to 0.99805 g/cm³), ρ_{vap} is the average density of water vapour in the system (equal to 0.0001 g/cm³), z is the distance from the centre of the water slab, z_0 is the interface in terms of the distance from the centre of the water slab, and ξ is the interface thickness. Table 1

gives the distance from the centre of the water slab and thickness of the interface for each partial pressure system. *n*-Hexane adsorption has only minor effects on the structure of the water film; the distance of the interface from the centre is reduced, at most, by 0.2%, and the interface thickness increases, at most, by 4% relative to neat water. In addition, changes in H-bonding on the interface were found to be less than 2%. These findings are consistent with the prior work of Pethica *et al.* [11], who also found no evidence of interface restructuring upon adsorption of alkanes.

4. Structure of adsorbed *n*-hexane

4.1. Density profiles across the interface

The location and boundaries of the water interface for the 95% partial pressure system are shown in Figure 2 alongside the density profiles for water and *n*-hexane. The densities of water are approximately 0.5, 0.15, and 0.85 g/cm³ at the centre, upper boundary, and lower boundary of the interface, respectively. In bulk water and up to the lower boundary of the interface, the *n*-hexane density is negligible; very few insertions of *n*-hexane into the bulk were accepted. The *n*-hexane density increases throughout the interface, and continues to increase beyond the upper boundary of the interface before decreasing to the bulk vapour density far from the interface.

The *n*-hexane density profiles for each system are compared in Figure 2. The density of *n*-hexane at the interface increases and reaches a maximum of 0.174 g/cm³ as the *n*-hexane partial pressure increases from 25% to 95%. For comparison, this local density is nearly a quarter the density of liquid *n*-hexane and 170 times the density of the corresponding vapour phase. Profile shapes remain about the same across all partial pressures, with a maximum density approximately 2\AA above the interface.

4.2. Orientation of *n*-hexane molecules in the adsorbed layer

The S_{CD} order parameter is a measure of the anisotropy of a particular C-D, or carbon-deuterated, bond that yields its time-averaged (ensemble) orientation in NMR experiments and has been used to characterise the orientational distribution of phospholipid bilayers [28,29] and liquid crystals [30,31]. In the present work, the order parameter (S) is computed according to Equation (3):

$$S = 0.5(3 \cos^2 \theta - 1), \quad (3)$$

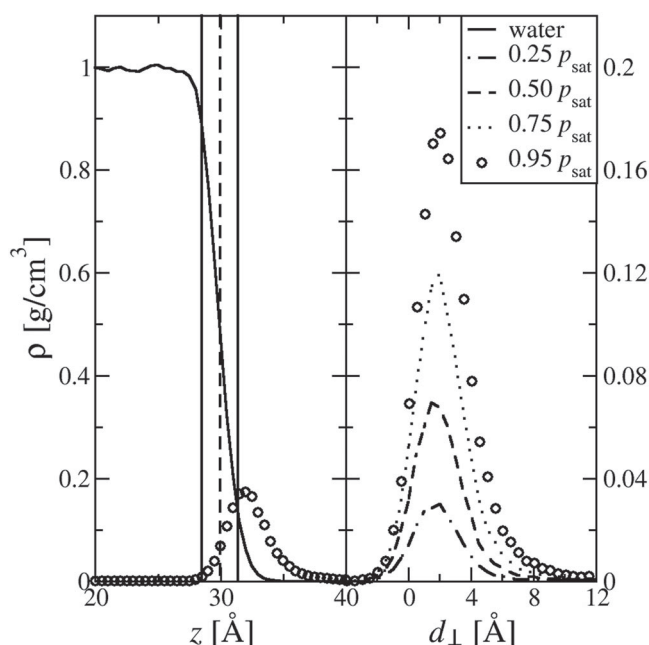


Figure 2. Density profiles of the water film and *n*-hexane at $0.95p_{\text{sat}}$ (left). The location of the interface, z_0 , and the interface thickness, ξ , are shown as dashed and solid vertical lines, respectively. Density profiles of *n*-hexane from $p/p_{\text{sat}} = 0.25$ to $p/p_{\text{sat}} = 0.95$ (right).

where θ is the angle formed between a vector along the z -axis (normal to the interface) and a vector formed between beads separated by two bonds. *n*-Hexane has six beads, resulting in a molecules' order parameter is the average of the contributions from 4 vectors. The value of S ranges from 1 when all molecules are oriented perpendicular to the interface to -0.5 when all molecules are oriented parallel to the interface; a value of 0 is observed for an ensemble of molecules with random orientation or for an ordered system with all molecules aligned along the magic angle. Figure 3 shows *n*-hexane's order parameter, S , as a function of distance, d_{\perp} , relative to the interface, z_0 (averaged for regions with a thickness of 1 Å). Near the interface ($-2 \text{ AA} < d_{\perp} < 4 \text{ AA}$), the order parameter is smaller than -0.1 for all four partial pressures, and the minimum in S is found for the region located at $d_{\perp} = 0.5 \text{ AA}$. The slight preference for parallel orientations permits the *n*-hexane molecules to increase the number of favorable contacts (i.e. negative Lennard–Jones water–hexane interaction energy) without severely disrupting the water–water interactions. Further above the interface, *n*-hexane molecules loose their preferential orientation, and $S = 0$ (within statistical uncertainties) is observed for $d_{\perp} > 6 \text{ AA}$. Throughout the simulations, too few *n*-hexane molecules are found at $d_{\perp} < 4 \text{ AA}$ to allow for calculation of the z -dependent order parameter. Interestingly, the S value is slightly positive for *n*-hexane molecules with their

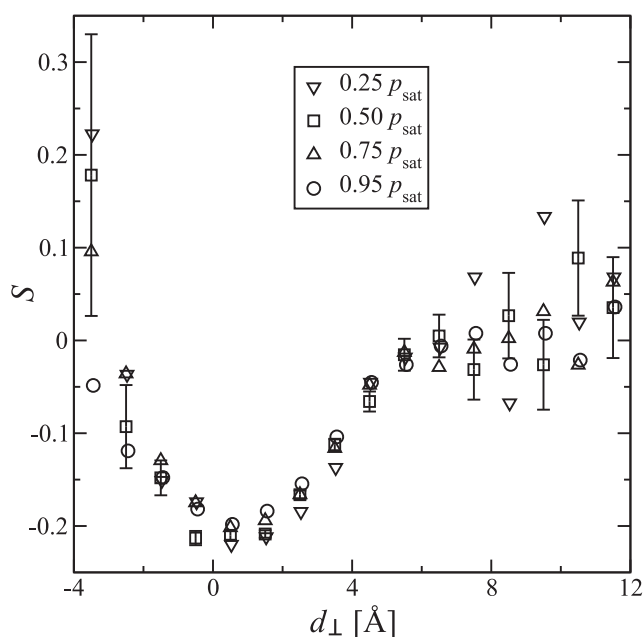


Figure 3. Orientation of *n*-hexane molecules in the adsorbed layer, measured by the order parameter, S , averaged over regions with a thickness of 1 Å as a function of distance, d_{\perp} , from the interface for $p/p_{\text{sat}} = 0.25$ to $p/p_{\text{sat}} = 0.95$. For clarity, error bars are only shown for the intermediate pressure.

center-of-mass located at $-4 \text{ AA} < d_{\perp} < -3 \text{ AA}$; the slight preference for perpendicular orientations arises from molecules that are partially submerged but with a minimum number of hydrophobic contacts.

4.3. Free energy profiles in the adsorbed phase

The partition function, $K(z)$, of the local density along the z -dimension over the bulk vapour density was obtained using Equation (4),

$$K(z) = \frac{\rho_{\text{H}}^{\text{L}}(z)}{\rho_{\text{H}}^{\text{V}}}, \quad (4)$$

where $\rho_{\text{H}}^{\text{L}}(z)$ is the local *n*-hexane density as a function of z in the interface box and $\rho_{\text{H}}^{\text{V}}$ is the *n*-hexane density in the vapour reservoir. This enables the calculation of the free energy of transfer as a function of z using Equation (5),

$$\Delta G(z) = -RT \ln(K(z)). \quad (5)$$

The $K(z)$ and $\Delta G(z)$ from $p/p_{\text{sat}} = 0.25$ to $p/p_{\text{sat}} = 0.95$ are shown in Figure 4.

Far from the interface, $K(z)$ for each partial pressure system approaches 1, and $\Delta G(z)$ approaches 0, indicating that this region of the interface box reaches the density of bulk *n*-hexane in the vapour reservoir. This demonstrates that the interface box is large enough to contain a

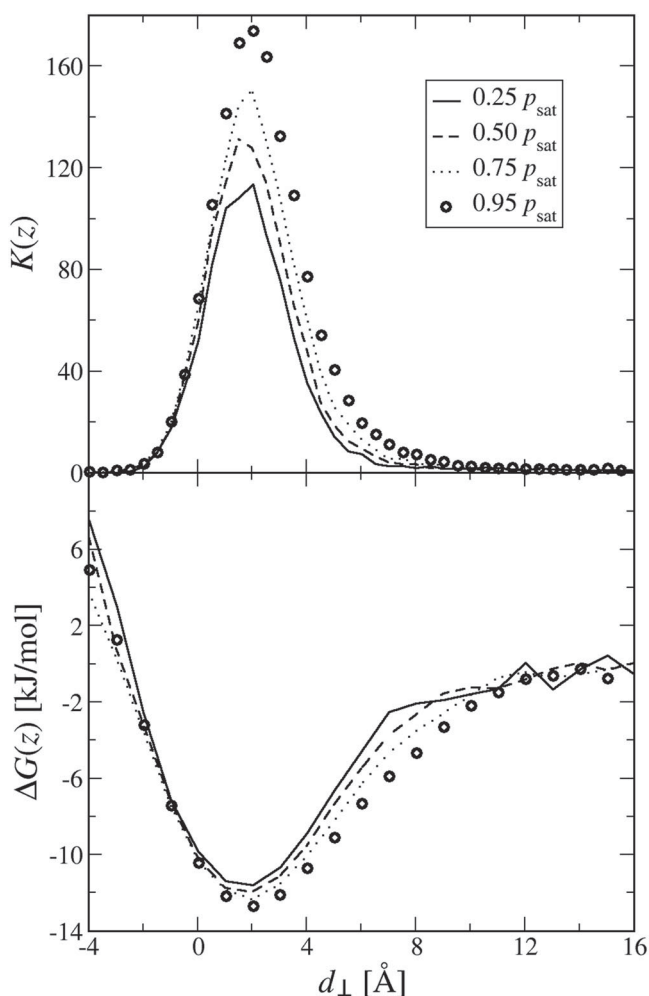


Figure 4. $K(z)$ from $p/p_{\text{sat}} = 0.25$ to $p/p_{\text{sat}} = 0.95$, as a function of distance from the interface, z_0 (top). Local free energy of transfer from vapour as a function of distance from the interface, z_0 (bottom).

domain of bulk vapour, so that the interfaces on opposite sides of the water film do not interact through periodic boundaries. It also shows that the simulation achieved an adequate number of MC cycles to reach equilibrium. In the bulk water where $d_{\perp} < -3 \text{ \AA}$, $K(z)$ and $\Delta G(z)$ show highly unfavourable adsorption of n -hexane relative to the vapour reservoir. This is in agreement with the low solubility of n -hexane in water. Near the interface, $K(z)$ increases and $\Delta G(z)$ decreases rapidly, until each reaches an extremum where n -hexanes are most densely populated, showing n -hexane interacts favourably at the interface. As partial pressure increases, $\Delta G(z)$ becomes more negative, from -11.7 to -12.7 kJ/mol from 25% to 95% p_{sat} , indicating cooperative hexane-hexane interactions that enhance adsorption. These cooperative hydrophobic interactions are relatively weak ($\sim 1 \text{ kJ/mol}$) compared to the interaction between the interface and the adsorbed n -hexane molecules ($\sim 11 \text{ kJ/mol}$), contradicting the

common notion that alkanes interact weakly with water relative to themselves.

5. Gibbs adsorption isotherm

The Gibbs adsorption isotherm characterises the change in surface tension of an interface as a molecule is adsorbed. For a binary system, the Gibbs isotherm is described by Equation (6),

$$-d\gamma = \Gamma_1 d\mu_1 + \Gamma_2 d\mu_2 \quad (6)$$

in which the change in surface tension $d\gamma$, arises from changes in the surface excess Γ_i and the chemical potential μ_i of each component. Because the n -hexane mole fraction in the liquid film is negligible, the chemical potential of water is essentially constant, leaving only one term in the Gibbs isotherm equation. To evaluate this relationship for the n -hexane/water system, we begin by computing the surface excess, Γ_{H} , using Equation (7),

$$\Gamma_{\text{H}} = N_{\text{H}}^{\text{ex}}/2A = (N_{\text{H}}^{\text{I}} - \rho_{\text{H}}^{\text{V}}V^{\text{I,V}} - \rho_{\text{H}}^{\text{L}}V^{\text{I,L}})/2A, \quad (7)$$

where N_{H}^{I} and N_{H}^{ex} are the total and excess numbers of n -hexane in the interface box, $V^{\text{I,V}}$ and $V^{\text{I,L}}$ are the volumes of vapour and liquid in the regions of the interface box defined according to z_0 , $\rho_{\text{H}}^{\text{V}}$ and $\rho_{\text{H}}^{\text{L}}$ are the densities of n -hexane in the vapour phase reservoir and in the bulk region of the liquid slab (calculated by computing the n -hexane density within the interior 50 \AA of the liquid slab), and A is the surface area (multiplied by 2 to account for both interfaces in the simulation box). Numerical values of N_{H}^{ex} are compared to the total N_{H}^{I} in Table 2.

Figure 5 shows the surface excess of n -hexane, Γ_{H} , as a function of the partial pressure of n -hexane. The surface excess at the lowest partial pressure, $0.25p_{\text{sat}}$, is used to calculate the Henry's constant and yields a value of $K_{\text{H}} = 0.616 \pm 0.008 \text{ molec/nm}^2$. At higher partial pressures, positive deviations from the Henry's slope are observed that indicate favourable adsorbate-adsorbate interactions. Figure 5 also shows data for the relation between the change in surface tension and the surface excess of n -hexane. Within the statistical errors (large for $\Delta\gamma$, but small for Γ_{H}), these data can be well described by a linear fit (correlation coefficient of $R^2 = 0.84$) and, hence, Equation (6) is found to hold for the water/ n -hexane interface.

6. Thermodynamics of adsorption

The free energy of transfer between two phases is calculated using the ratio of number densities between the

Table 2. Total number of *n*-hexane molecules in the interface box, the number of excess *n*-hexane molecules calculated with Equation (7), the upper and lower bounds of integration as optimised by Equation (8), and free energies, enthalpies, and entropies of adsorption calculated with Equations (9) and (10).

	N_{H}^{I} (molec)	N_{H}^{ex} (molec)	Upper and lower bounds of integration (Å)	ΔG_{ads} (kJ/mol)	ΔH_{ads} (kJ/mol)	$T\Delta S_{\text{ads}}$ (kJ/mol)
$0.25p_{\text{sat}}$	1.49 ₂	1.39 ₂	-2.0 ↔ 6.5	-9.56 ₃	-29 ₄	-19 ₄
$0.50p_{\text{sat}}$	3.50 ₃	3.29 ₃	-2.0 ↔ 7.0	-9.84 ₂	-24 ₂	-14 ₂
$0.75p_{\text{sat}}$	6.06 ₄	5.76 ₄	-2.0 ↔ 7.5	-10.07 ₂	-21 ₁	-10 ₁
$0.95p_{\text{sat}}$	9.21 ₆	8.82 ₆	-2.0 ↔ 8.0	-10.40 ₂	-21.1 ₁	-10.7 ₈
$0.95p_{\text{sat}}^*$	6.40 ₂	6.01 ₂	-1.5 ↔ 8.0	-9.59 ₁	-20.6 ₆	-11.0 ₆
Liquid <i>n</i> -Hexane	-	-	-	-15.816 ₇	-28.882 ₃	-13.065 ₈

Notes: The free energy and enthalpy of condensation for liquid *n*-hexane is also calculated using a two box Gibbs ensemble simulation at 297 K, enabling the calculation of the entropy of condensation from Equation (9). *Computed using LB σ_{ij} and ϵ_{ij} instead of HH σ_{ij} and ϵ_{ij} .

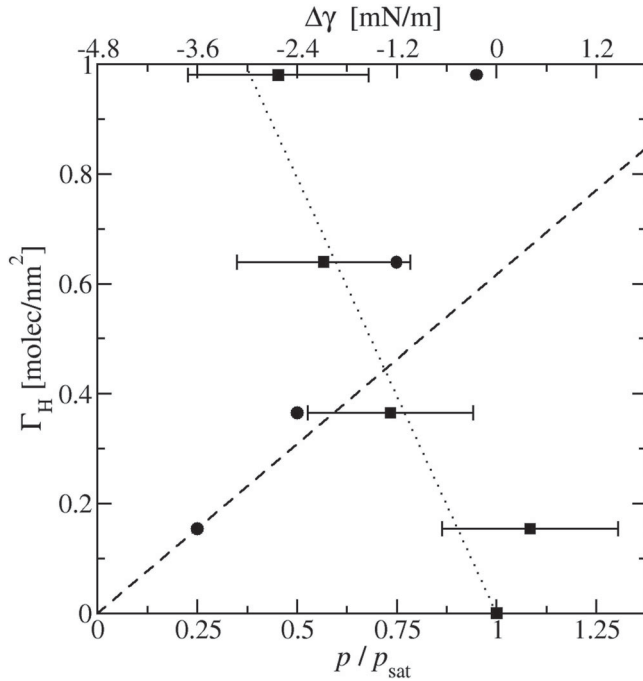


Figure 5. The surface excess of *n*-hexane, calculated with Equation (7), versus the change in surface tension (top x-axis) and the partial pressure of *n*-hexane vapour (bottom x-axis). The square symbols and dotted black line correspond to the change in surface tension, and the circle symbols and dashed black line correspond to the partial pressure.

phases (Equation (9)). In a simulation box containing distinct regions for bulk water, bulk vapour, and an interface, the domain corresponding to the adsorbed phase must be defined to compute its density and the corresponding free energy of adsorption. A suitable definition for the ‘region of adsorbed *n*-hexane’ is the smallest region containing all excess adsorbed molecules, N_{H}^{ex} as calculated by Equation (7). In practice, the density profiles of Figure 2 are numerically integrated using Simpson’s Rule, with lower and upper bounds chosen to minimise the volume of the integrated region subject to the constraint that the number of *n*-hexane molecules in the

integrated region is greater or equal to the number of excess *n*-hexane (Equation (8)).

$$\text{minimise } V^{\text{ads}} = (b - a)A$$

$$\text{subject to } N_{\text{H}}^{\text{ads}} = \int_a^b \rho_{\text{H}}^{\text{I}}(z) dz \geq N_{\text{H}}^{\text{ex}}. \quad (8)$$

The free energy of adsorption (Equation (9)), is then computed using the ratio of number densities of *n*-hexane between the vapour box and this ‘region of adsorbed *n*-hexane’. Table 2 gives the lower and upper bounds of this integration, and the corresponding ΔG_{ads} for each partial pressure as calculated using this method. The ‘region of adsorbed *n*-hexane’ begins slightly below z_0 and extends 6.5–8.0 Å above z_0 , giving typical volumes approximately 1/6 of the volume of the interface box, while containing 93–96% of the *n*-hexane molecules in the box. This substantially improves the estimate of ΔG_{ads} compared to a naive calculation using the ΔG of transfer between the vapour reservoir and the entire interface box, which underestimates the magnitude of ΔG_{ads} by 5 kJ/mol.

$$\Delta G_{\text{ads}} = -RT \ln \frac{\rho_{\text{H}}^{\text{ads}}}{\rho_{\text{H}}^{\text{V}}} = \Delta H_{\text{ads}} - T\Delta S_{\text{ads}}. \quad (9)$$

The relative contributions of enthalpy and entropy of adsorption were decoupled from the free energy using Equation (10),

$$\begin{aligned} \Delta H_{\text{ads}} &= \Delta E_{\text{ads}} + P\Delta V_{\text{ads}} = E_{\text{H+W}}^{\text{I}} - E_{\text{W}}^{\text{I}} - \frac{E_{\text{H}}^{\text{V}}}{N_{\text{H}}^{\text{V}}} N_{\text{H}}^{\text{I}} \\ &\quad + P \frac{V_{\text{H}}^{\text{V}}}{N_{\text{H}}^{\text{V}}} N_{\text{H}}^{\text{I}} \\ \Delta H_{\text{ads}} &= \frac{E_{\text{H+W}}^{\text{I}}}{N_{\text{H}}^{\text{I}}} - \frac{E_{\text{W}}^{\text{I}}}{N_{\text{H}}^{\text{I}}} - \frac{E_{\text{H}}^{\text{V}}}{N_{\text{H}}^{\text{V}}} + \frac{V_{\text{H}}^{\text{V}}}{N_{\text{H}}^{\text{V}}}, \end{aligned} \quad (10)$$

where the internal energy of adsorption, ΔE_{ads} , is computed from the difference of average total energy between

the interface box with *n*-hexane adsorbed, E_{H+W}^I , and the average total energy of the neat water film, E_W^I , and the vapour-phase energy, E_H^V/N_H^V , of the transferred *n*-hexane molecules, N_H^I . The pressure-volume contribution is calculated using the system pressure, p_H , and the molar volume of the vapour, V_H^V/N_H^V . Dividing by N_H^I gives the ΔH_{ads} on a molar basis. Subtracting ΔG_{ads} from ΔH_{ads} leads to the entropic contribution to the free energy. These relevant quantities are given in Table 2. Equation (10) is useful for computing the enthalpy of adsorption without explicitly re-calculating the interactions of the molecules in the ‘region of adsorbed *n*-hexane’. Note that Equation (10) assumes that water is constrained to the liquid phase and does not contribute to the energy or volume of the vapour reservoir. Equation (10) also neglects to account for the difference in internal energy between the *n*-hexane molecules in the ‘region of adsorbed *n*-hexane’ compared to that of the *n*-hexane in the bulk water or the vapour domains of the interface box, which is a reasonable approximation when 93–96% of *n*-hexane are in the adsorbed region.

The free energy of adsorption is negative, indicating an enrichment of *n*-hexane in the interface relative to the vapour phase. Enthalpy of adsorption is also negative, indicating that the interactions in the interface are more energetically favourable than in the vapour phase. The entropy of adsorption is also negative, because *n*-hexane molecules lose translational and rotational degrees of freedom when they adsorb and align onto the interface. As partial pressure increases from 25% to 95% p_{sat} , both enthalpic and entropic contributions decrease in magnitude. The enthalpy of adsorption is more negative at low partial pressure, where *n*-hexane molecules align closer to the interface and interact more strongly with the water. In all cases, ΔG_{ads} onto the water interface is less favourable than condensation to liquid *n*-hexane, but still much more favourable than remaining in the vapour phase. In addition, near the saturation pressure, ΔH_{ads} is less favourable than the enthalpy of condensation into liquid *n*-hexane, indicating that *n*-hexane prefers to be in the liquid phase.

7. Conclusions

Using MC simulations in the osmotic Gibbs ensemble, we simulated adsorption of *n*-hexane onto the surface of liquid water. This adsorption is associated with a reduction in surface tension of the interface, in agreement with experimental observations and expectations from the Gibbs adsorption isotherm model. The density of *n*-hexane on the interface increases with increasing partial pressure, with a positive deviation from Henry’s Law

at higher partial pressures. This, as well as a decrease in ΔG_{ads} at higher partial pressures, provides evidence for cooperative hexane-hexane interactions. After decoupling the free energy, enthalpy, and entropy of adsorption, we determine that the adsorption of *n*-hexane vapour onto the interface is enthalpically driven by the water–hexane interactions. This leads to preferential ordering of *n*-hexane molecules parallel to the interface. The methods used here would be applicable for extending this work to study adsorption behaviour in other vapour/liquid/interfacial systems.

Acknowledgments

We thank David Harwood for helpful comments.

Disclosure statement

There is no potential conflict of interest for this work.

Funding

This collaborative research was supported by the Abu Dhabi Petroleum Institute Research Center (Project Code LTR14009) and the University of Minnesota Disability Resource Center through access assistants to Dr Minkara; specifically, Tanner Lambson, Tyler Westland, and John Hamill. A portion of the computer resources were provided by the Minnesota Supercomputing Institute at the University of Minnesota.

ORCID

Mona S. Minkara  <http://orcid.org/0000-0003-1821-2725>
 Tyler Josephson  <http://orcid.org/0000-0002-0100-0227>
 Daniel J. Stein  <http://orcid.org/0000-0002-9442-2604>
 Cor J. Peters  <http://orcid.org/0000-0001-8083-0503>
 J. Ilja Siepmann  <http://orcid.org/0000-0003-2534-4507>

References

- [1] E. Bertrand, D. Bonn, D. Broseta, H. Hobbs, J.O. Indekeu, J. Meunier, K. Ragil, and N. Shahidzadeh, *J. Pet. Sci. Eng.* **33**, 217 (2002).
- [2] N. Shahidzadeh, E. Bertrand, J.P. Dauplat, J.C. Borgotti, P. Vié, and D. Bonn, *Transp. Porous Media* **52**, 213 (2003).
- [3] V. Bergeron, D. Bonn, J.Y. Martin, and L. Vovelle, *Nature* **405**, 772 (2000).
- [4] B.A. Pethica, *Langmuir* **12**, 5851 (1996).
- [5] A. Lou and B.A. Pethica, *Langmuir* **13**, 4933 (1997).
- [6] P. Chen, S.S. Susnar, A. Amirfazli, C. Mak, and A.W. Neumann, *Langmuir* **13**, 3035 (1997).
- [7] H. Dobbs, *Langmuir* **15**, 2586 (1999).
- [8] R. Aveyard, J.H. Clint, D. Nees, and V. Paunov, *Colloids Surf. A* **146**, 95 (1999).
- [9] H. Dobbs, *Langmuir* **16**, 4749 (2000).
- [10] H.S. Ashbaugh and B.A. Pethica, *Langmuir* **19**, 7638 (2003).

- [11] B.A. Pethica, M.L. Glasser, and E.H. Cong, *Langmuir* **19**, 6820 (2003).
- [12] B.A. Pethica and M.L. Glasser, *Langmuir* **21**, 944 (2005).
- [13] S. Rafai, D. Bonn, and J. Meunier, *Phys. A* **358**, 197 (2005).
- [14] H. Matsubara, M. Aratono, K.M. Wilkinson, and C.D. Bain, *Langmuir* **22**, 982 (2006).
- [15] A. Javadi, N. Moradi, H. M \ddot{o} hwald, and R. Miller, *Soft Matter* **6**, 4710 (2010).
- [16] N. Mucic, N. Moradi, A. Javadi, E.V. Aksenenko, V.B. Fainerman, and R. Miller, *Colloids Surf. A* **442**, 50 (2014).
- [17] N. Mucic, N. Moradi, A. Javadi, E.V. Aksenenko, V.B. Fainerman, and R. Miller, *Colloids Surf. A* **480**, 79 (2015).
- [18] A.R. van Buuren, S.J. Marrink, and H.J.C. Berendsen, *J. Phys. Chem.* **97**, 9206 (1993).
- [19] J.L. Chen, B. Xue, D.B. Harwood, Q.P. Chen, C.J. Peters, and J.I. Siepmann, *Fluid Phase Equilib.* (2018). doi:10.1016/j.fluid.2017.06.015.
- [20] M.G. Martin and J.I. Siepmann, *J. Phys. Chem. B* **102**, 2569 (1998).
- [21] J.L.F. Abascal and C. Vega, *J. Chem. Phys.* **123**, 234505 (2005).
- [22] R. Span, *Multiparameter Equations of State – An Accurate Source of Thermodynamic Property Data* (Springer, Berlin, 2000), p. 367.
- [23] C. Vega, J.L.F. Abascal, and I. Nezbeda, *J. Chem. Phys.* **125**, 034503 (2006).
- [24] J. Janeček, *J. Phys. Chem. B* **110**, 6264 (2006).
- [25] J.G. Kirkwood and F.P. Buff, *J. Chem. Phys.* **17**, 338 (1949).
- [26] A. Ghoufi, P. Malfret, and D.J. Tildesley, *Chem. Soc. Rev.* **45**, 1387 (2016).
- [27] H.S. Ashbaugh, L. Liu, and L.N. Surampudi, *J. Chem. Phys.* **135**, 054510 (2011).
- [28] O. Berger, O. Edholm, and F. Jähnig, *Biophys. J.* **72**, 2002 (1997).
- [29] H. Schindler and J. Seelig, *Biochemistry* **14**, 2283 (1975).
- [30] S. Marčelja, *J. Chem. Phys.* **60**, 3599 (1974).
- [31] S. Marčelja, *Biochim. Biophys. Acta* **367**, 165 (1974).